Reorientational and configurational fluctuations in water observed on molecular length scales

J. J. Loparo, C. J. Fecko, J. D. Eaves, S. T. Roberts, and A. Tokmakoff

Department of Chemistry and George R. Harrison Spectroscopy Laboratory, Massachusetts Institute of Technology, Cambridge, Massachusetts 02139, USA

Polarization-selective pump-probe and echo experiments on the OH vibration of HOD in D_2O with 45-femtosecond (fs) infrared pulses are analyzed self-consistently to reveal the time scales for vibrational relaxation, dephasing, and molecular reorientation. Librational motion and hydrogen bond fluctuations on 50- and 180-fs time scales precede picosecond collective reorganization.

PACS number(s): 78.30.Cp, 78.47.+p

The unique physical and chemical properties of water originate from the hydrogen bond rearrangements that make transient intermolecular geometries appear, fluctuate, and disappear. Since the early 1970's, researchers have used molecular-dynamics (MD) simulations to explore the connection between hydrogen bonding interactions and the bulk and transport properties of water. The work of Rahman and Stillinger explained much of the available experimental data for liquid water with classical mechanics on simple empirical potentials.[1] Inspired by these models, researchers have applied them to elucidate the microscopic mechanisms of hydrogen bond breaking and forming. These studies have found that intermolecular dynamics span time scales from roughly 50 femtoseconds for motions on molecular length scales, to picoseconds for cooperative molecular reorganization of the liquid. It is only recently, with the ability to generate optical and infrared pulses that are faster than the intermolecular motions of water, that femtosecond spectroscopies have been able to experimentally probe the dynamics of water molecules and hydrogen bonds. Here, we present a unified analysis of infrared vibrational echo and polarization-selective pump-probe (PP) experiments that reveal the short-time molecular reorientation and hydrogen bond dynamics in water prior to collective reorganization. This provides experimental data for comparison with predictions from molecular-dynamics simulations based on empirical classical potentials.

Infrared spectroscopy is an ideal technique to study hydrogen bonding liquids, because the frequency of the OH stretch is sensitive to the hydrogen bonded environment. Spectroscopists have commonly used an isotopically dilute sample of HOD in D_2O as a model system because the OH vibration is a localized probe, free of vibrational coupling between neighboring OH oscillators that complicates the spectroscopy of pure water. Recent molecular-dynamics studies have shown that there is a fairly strong correlation between the OH frequency of HOD in D_2O and the $O—H \cdots O$ hydrogen bond length.[2–4] However, the angular variation of hydrogen bonds in the liquid reduces this correlation. More generally, we have shown that the molecular electric field at the proton in the direction of the OH bond vector determines the frequency ω.[4] The configuration of the hydrogen bond acceptor molecule with respect to the OH bond determines the majority of the field strength. Structural evolution of the hydrogen bonding network changes the electric field felt by the OH oscillator and results in time-

dependent shifts in the OH stretching frequency $\delta\omega(t)$. Transient infrared spectroscopy is capable of measuring these OH frequency shifts, or spectral diffusion. The characteristic time scales and amplitudes of spectral diffusion can then be related to hydrogen bond configurational changes and reorganization of the hydrogen bonding network.

In most studies to date, spectrally narrow pulses have excited a part of the OH absorption line shape of HOD in D_2O and the relaxation of this subensemble was probed as it reequilibrated.[5–7] These transient hole burning (THB) experiments have characterized subpicosecond time scales, but the narrow spectral bandwidth required in these measurements has limited the time resolution to roughly 150 fs. This prevented them from observing water's fastest intermolecular motions. Vibrational echo experiments have accessed the sub- 100-fs time scales of spectral diffusion in water, although with varying results.[4,8–12] Our vibrational echo peak shift (PS) measurement with 50-fs pulses, shown in Fig. 1(a), has a rapid 60-fs decay and a weak beat peaking at 160-fs, before dropping into a 1.2-ps decay.[4] We now report a series of polarization-dependent PP experiments with even shorter pulses, which show new signatures of librational motions predicted by MD simulations and further support the observation of underdamped hydrogen bond motion. A self-consistent modeling of the PP and the PS data yields three dynamical quantities that provide a quantitative description of spectral diffusion, vibrational population relaxation, and molecular reorientation: $C(\tau)$, T_1, and $p_2(\tau)$. The OH frequency autocorrelation function is $C(\tau)=\langle\delta\omega(\tau)\delta\omega(0)\rangle$, $1/T_1$ is the rate for relaxation of the OH vibration, and $p_2(\tau)$ $=\langle P_2(\hat{\mu}(\tau)\cdot\hat{\mu}(0))\rangle$ is the second Legendre polynomial of the reorientational correlation function for the unit vector of the OH transition dipole. Because the short temporal duration of the excitation pulse provided enough frequency bandwidth to span the fundamental and most of the anharmonically shifted overtone of the OH stretch of HOD/D_2O, these pulses averaged over all molecular environments. These measurements allow for direct comparison of the IR spectroscopy of HOD/D_2O to models and simulations of vibrational dephasing, lifetime, and reorientation based on correlation functions.

Experiments used 45-fs pulses generated with a dual stage BBO/$KNbO_3$ optical parametric amplifier pumped by a 30-fs Ti:sapphire amplifier. The pulses typically had a
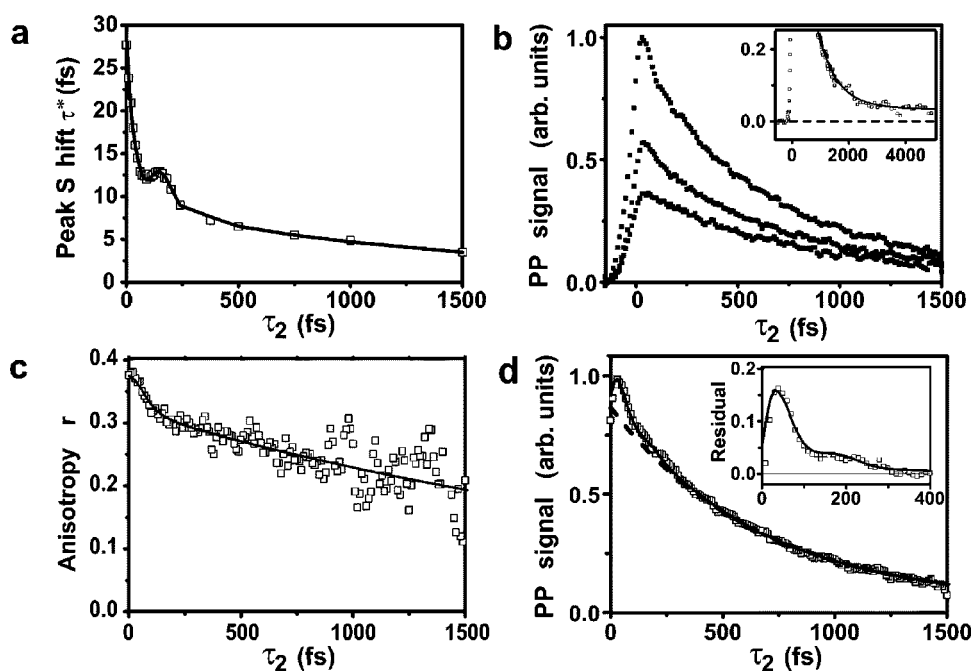
FIG. 1. Data are represented as points while fits from a unified analysis of the data are solid lines. (a) The vibrational echo peak shift. (b) Polarization-selective pump-probe. $S_\parallel$, S_{MA}, and $S_\perp$ are shown from top to bottom. The inset shows the offset present in the long-time tail of the pump-probe signal. (c) Anisotropy $r(\tau)$ determined from $S_\parallel$ and $S_\perp$. (d) $S_\parallel$ with exponential fit to the long-time tail. The inset shows the residual when the exponential fit is subtracted from the data.

spectral bandwidth of 400 cm^{-1} with flat spectral phase (<0.2 rad variation) when characterized by SHG-FROG. The center frequency was set to 3300 cm^{-1} to span the entire fundamental absorption line shape and much of the anharmonically shifted $v=1 \rightarrow 2$ transition. The sample was an HOD in D$_2$O water jet formed by a 50-μm sapphire nozzle with a total peak optical density of ~0.4. We have found that experiments taken in sample cells show a strong nonresonant response from the cell window that masks the short-time dynamics observed in the jet. The polarization of the beams was controlled with wire-grid polarizers. Data was acquired by measuring the pump-induced transmission change on the probe pulse, normalized to the transmission of a third reference pulse. To reduce $v=2$ induced absorption signals in PP experiments, the transmitted probe beam passed through a 50-cm^{-1} bandpass filter centered at line center (3400 cm^{-1}) before detection.

Polarization-selective PP measurements can be used to separate the dynamics of reorientation from dephasing and lifetime relaxation. When combined with PS experiments, polarization-dependent PP experiments can isolate each contribution. Figure 1(b) shows PP measurements for parallel $S_\parallel$, perpendicular $S_\perp$, and magic angle S_{MA} polarization geometries. The polarization measurements differ in both the profile of the sub-500-fs transients and the time scales of their long-time decays. S_{MA} is free of reorientational effects and shows an asymptotic single exponential decay due to the OH lifetime with $T_1 = 700$ fs. This value can be compared with values of 650 (Ref. 6), 740 (Ref. 13), and 1000 fs (Ref. 7) from THB. On time scales long compared to T_1, PP measurements reveal a 3% percent offset [inset, Fig. 1(b)]. This offset is similar to long-time signals observed in IR THB and narrow-band PS experiments, which are ascribed to vibrational-relaxation-induced changes in the excitation of intermolecular motions leading to a "hot-ground-state" differential absorption signal.[9,13] This offset remains constant

for more than 50 ps, which is consistent with heating and reequilibration of the sample via thermal diffusion.

The reorientational correlation function of the OH dipole $p_2(\tau)$ is obtained from the parallel and perpendicular PP measurements through the anisotropy $r(\tau) = (S_\parallel - S_\perp)/(S_\parallel + 2S_\perp)$, shown in Fig. 1(c). The anisotropy has an initial value of 0.38, and decays biexponentially with 50-fs and 3-ps components. The 50-fs component has not been observed previously in IR measurements, but follows the time scale associated with molecular libration. The long-time component is similar to experimental time scales observed by IR hole burning and NMR.[14–16]

The influence of vibrational dephasing on the PP transient is apparent by subtracting the effects of reorientation and population relaxation, as shown in the inset of Fig. 1(d). This short-time transient should follow the correlation function for the system,[17] and shows a rapid decay followed by a weak recurrence at ~180 fs. This transient is similar to the short-time behavior of the PS measurement, and provides further evidence for underdamped modulation of the OH frequency during dephasing.

The PP and PS data can be described self-consistently with a third-order nonlinear response function $\bar{\mathbf{R}}^{(3)}$ that is expressed in terms of frequency correlation functions for the splitting between vibrational levels, the vibrational lifetime for $v=1$, and orientational correlation functions for the OH vector. The formalism is similar to methods we have described previously,[18] and draws on the multilevel nonlinear response function described by Sung and Silbey.[19] Full details of the analysis will be provided in a later publication. We account for vibrational relaxation phenomenologically by adding vibrational lifetimes for the different levels, while reorientation is expressed in terms of $p_1(\tau)$ and $p_2(\tau)$. Correlation functions for the energy gaps, the transition moments, and the vibrational lifetime involving the $v=2$ state are related to expressions involving $v=1$ through harmonic
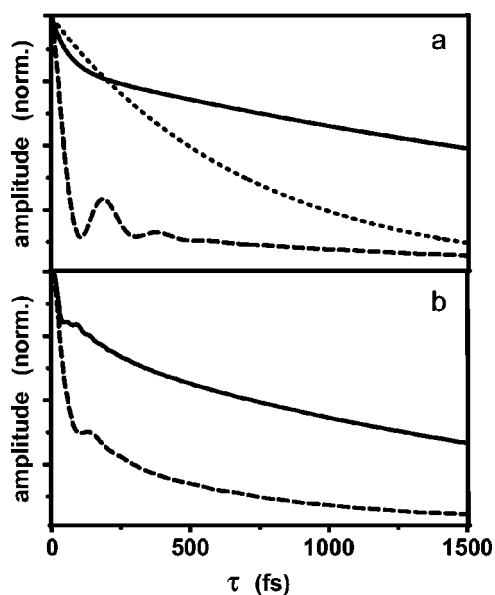
FIG. 2. (a) Plots of the normalized $C(\tau)$ (dashed), $p_2(\tau)$ (solid), and OH vibrational lifetime decay [$\exp(-\tau/T_1)$; dotted]. The zero-time amplitude of the correlation function was found to be $C(\tau)=5.7\times10^{-4}$ fs^{-2}. (b) $C(\tau)$ and $p_2(\tau)$ derived from MD simulation of HOD in D$_2$O using the SPC/E model for water Ref. 4. The long-time decays of $C(\tau)$ and $p_2(\tau)$ are 0.6 and 2.6 ps, respectively.

scaling relationships to reduce the number of free parameters. For the orientational correlation function we assume that the OH transition moments for $\boldsymbol{\mu}_{10}$ are parallel to $\boldsymbol{\mu}_{21}$, and use the scaling factor for diffusive orientation $p_1(\tau)=p_2(\tau/3)$. In order to account for the observed offset in the experimental data at times longer than the vibrational lifetime, we use a response function that accounts for spectroscopic changes on relaxing to a hot ground state. This approach is similar to schemes used to model previous experiments.[9,13] Good fits to both the long-time PS and the offset observed in the PP required a 12-cm^{-1} relaxation-induced blueshift in the fundamental transition energy and a 5% decrease in the transition moment. This is consistent with the spectral changes observed in Fourier transform infrared (FTIR) spectra of HOD in D$_2$O when the temperature increases. The experiments are simulated by convoluting $\bar{\mathbf{R}}^{(3)}$ with the electric field of the pulses, taking into account all possible time-ordered signal contributions into the wave-vector-matched direction. The solid lines plotted along with the data in Fig. 1 are the best fits obtained with this formalism. The fit reproduces the short, intermediate, and long-time features of the PS and PP data.

The underlying dynamics of vibrational dephasing, lifetime, and reorientation, expressed as $C(\tau)$, T_1, and $p_2(\tau)$, are shown in Fig. 2(a). From these quantities one can construct a picture of the underlying dynamics of water's hydrogen bonding network. The correlation time for frequency fluctuations of $\tau_C=340$ fs, calculated by integrating $C(\tau)$ and dividing by $C(0)$, serves as a convenient way to divide the dynamics. Times shorter than τ_C reflect the dynamics of structural fluctuations within relatively fixed intermolecular configurations, whereas longer time scales characterize the kinetics of collective configurational changes in the hydrogen bond network.

At short times the dynamics are dominated by two fast time scales: the 50-fs decay component of the reorientational correlation function and the underdamped oscillation with the 180-fs time period in the frequency correlation function. Both time scales are due to fast intermolecular motions that occur over molecular length scales. These reflect hindered rotations and translations, intermolecular fluctuations that, according to MD simulations, lead to hydrogen bond breaking.[20] The oscillatory behavior in $C(\tau)$ largely reflects the intermolecular motion between the HOD and the hydrogen bonding partner for the proton. While the OH frequency shift reflects the electric field of all D$_2$O molecules acting on the OH coordinate, the displacement and angular changes between the two molecules results in the dominant fluctuations of the molecular electric field projected onto the OH coordinate.[4] The oscillation shows that the hydrogen bond is not overdamped as previous IR THB studies had concluded.[5,6] The fast decay in $p_2(\tau)$ is consistent with the librational motion of water. Unlike Raman measurements that probe the many-body polarizability, the infrared measurement presented here is an observation of the hindered rotational motion of individual OH dipoles. The cosine transform of the frequency correlation function (not shown) has a very small contribution at 400 cm^{-1}, suggesting that librations do not contribute significantly to the rapid decay of the $C(\tau)$.

At times longer than τ_C, the frequency correlation function and the anisotropy decay on 1.4- and 3-ps time scales, respectively. As shown previously by MD simulations, a variety of relaxation mechanisms occur on the picosecond time scale including the collective rearrangement of the hydrogen bonding network, as well as density and polarization fluctuations on length scales greater than a molecular diameter. Contrary to the dynamics at early times that are well described by the OH oscillator and its hydrogen bonding partner, these processes involve the motions of many molecules and are therefore inherently collective. Molecular reorientation is also collective, occuring with the structural reorganization of the hydrogen bonding network as a molecule must break multiple hydrogen bonds to rotate. On a similar time scale of 700 fs, the combination of these intermolecular forces act on the OH coordinate, leading to fast vibrational relaxation.

The frequency and reorientational correlation functions presented here demonstrate remarkable agreement with over 30 years of MD simulations. In $C(\tau)$ we observe an oscillation corresponding to the intermolecular vibration in the oxygen velocity autocorrelation function for water,[2,21] calculated by Rahman and Stillinger. Likewise, Stillinger's calculation of $p_2(\tau)$ showed biexponential relaxation with comparable time scales to those measured by our experiment.[1] Only recently have MD simulations attempted to calculate the frequency correlation function for the OH stretch.[2–4] Figure 2(b) shows simulation results for $C(\tau)$ and $p_2(\tau)$ of HOD in D$_2$O derived from the SPC/E model for water. Calculations like these, by Lawrence and Skinner, give similar results regarding the fast and slow time scales.[3] The qualitative

agreement between simulation and experiment indicates that relatively simple fixed-point charge water potentials capture the essential reorientational and dephasing dynamics measured in the present experiments. The fact that the experimental time scales are consistently longer than those obtained from this model argue that more sophisticated models for the intermolecular interactions in water could lead to better quantitative agreement. For instance, including polarizable effects, where molecular charges respond dynamically to the environment, show slower reorientational diffusion and hydrogen bond breaking times.[22]

The vibrational and orientational motions reported here represent an average over all possible initial intermolecular configurations, each of which may in fact experience different dynamical environments on subtly different time scales. While there is evidence that subensemble dynamics are spectrally heterogeneous,[11,12,23] we have made approximations in our analysis that do not describe a heterogeneous system. Specifically, our model assumes the fluctuations are Gauss-

ian, and does not properly treat systems where molecules prepared on the red or blue side of the OH lineshape relax differently. Nonetheless, our observation of a fast correlation time τ_c and simple exponential relaxation on longer time scales suggest a small degree of heterogeneity in reorientation and lifetime on picosecond time scales. This is consistent with the finding of two-dimensional infrared spectroscopy of vibrational dynamics in H_2O.[11,12] Our analysis provides an averaged description of hydrogen bonding dynamics within the traditional pictures of spectroscopy, and gives a self-consistent description of the many time-dependent relaxation phenomena of HOD in D_2O.

[1] A. Rahman and F. H. Stillinger, J. Chem. Phys. **55**, 3336 (1971).

[2] R. Rey, K. B. Moller, and J. T. Hynes, J. Phys. Chem. A **106**, 11993 (2002).

[3] C. P. Lawrence and J. L. Skinner, J. Chem. Phys. **118**, 264 (2003).

[4] C. J. Fecko *et al.*, Science **301**, 1698 (2003).

[5] S. Woutersen and H. J. Bakker, Phys. Rev. Lett. **83**, 2077 (1999).

[6] G. M. Gale *et al.*, Phys. Rev. Lett. **82**, 1068 (1999).

[7] R. Laenen, K. Simeonidis, and A. Laubereau, J. Phys. Chem. B **106**, 408 (2002).

[8] J. Stenger, D. Madsen, P. Hamm, E. T. J. Nibbering, and T. Elsaesser, Phys. Rev. Lett. **87**, 027401 (2001).

[9] J. Stenger *et al.*, J. Phys. Chem. A **106**, 2341 (2002).

[10] S. Yeremenko, M. S. Pshenichnikov, and D. A. Wiersma, Chem. Phys. Lett. **369**, 107 (2003).

[11] T. Steinel *et al.*, Chem. Phys. Lett. **386**, 295 (2004).

[12] J. B. Asbury *et al.*, J. Phys. Chem. A **108**, 1107 (2004).

[13] H. K. Nienhuys *et al.*, J. Chem. Phys. **111**, 1494 (1999).

[14] G. Gallot *et al.*, J. Chem. Phys. **117**, 11301 (2002).

[15] D. W. G. Smith and J. G. Powles, Mol. Phys. **10**, 451 (1966).

[16] H.-K. Nienhuys, R. A. van Santen, and H. J. Bakker, J. Chem. Phys. **112**, 8487 (2000).

[17] D. A. Farrow, A. Yu, and D. M. Jonas, J. Chem. Phys. **118**, 9348 (2003).

[18] M. Khalil, N. Demirdöven, and A. Tokmakoff, J. Phys. Chem. A **107**, 5258 (2003).

[19] J. Sung and R. J. Silbey, J. Chem. Phys. **115**, 9266 (2001).

[20] A. Luzar and D. Chandler, Phys. Rev. Lett. **76**, 928 (1996).

[21] U. Balucani, J. P. Brodholt, and R. Vallauri, J. Phys.: Condens. Matter **8**, 6139 (1996).

[22] H. Xu, H. A. Stern, and B. J. Berne, J. Phys. Chem. B **106**, 2054 (2002).

[23] S. Woutersen, U. Emmerichs, and H. J. Bakker, Science **278**, 658 (1997).